

10-2017

A Near-Global Atmospheric Distribution of N₂O Isotopologues

Peter F. Bernath

Old Dominion University, pbernath@odu.edu

Mahdi Yousefi


Old Dominion University

Eric Buzan

Old Dominion University

Chris D. Boone

Follow this and additional works at: https://digitalcommons.odu.edu/chemistry_fac_pubs

 Part of the [Atmospheric Sciences Commons](#), [Chemistry Commons](#), and the [Geochemistry Commons](#)

Repository Citation

Bernath, Peter F.; Yousefi, Mahdi; Buzan, Eric; and Boone, Chris D., "A Near-Global Atmospheric Distribution of N₂O Isotopologues" (2017). *Chemistry & Biochemistry Faculty Publications*. 101.
https://digitalcommons.odu.edu/chemistry_fac_pubs/101

Original Publication Citation

Bernath, P. F., Yousefi, M., Buzan, E., & Boone, C. D. (2017). A near-global atmospheric distribution of N₂O isotopologues. *Geophysical Research Letters*, 44(20), 10735-10743. doi:10.1002/2017gl075122

RESEARCH LETTER

10.1002/2017GL075122

Key Points:

- Near-global observations of atmospheric NNO, ^{15}NNO , N^{15}NO , and NN^{18}O were made with ACE satellite
- Isotopic fractionation was modeled with WACCM
- Relative stratospheric abundances of the heavier isotopologues and isotopomers are enhanced at higher altitudes and over the poles

Supporting Information:

- Data Set S1
- Data Set S2
- Supporting Information S1

Correspondence to:

P. F. Bernath,
pbernath@odu.edu

Citation:

Bernath, P. F., Yousefi, M., Buzan, E., & Boone, C. D. (2017). A near-global atmospheric distribution of N_2O isotopologues. *Geophysical Research Letters*, 44, 10,735–10,743. <https://doi.org/10.1002/2017GL075122>

Received 28 JUL 2017

Accepted 6 OCT 2017

Accepted article online 12 OCT 2017

Published online 28 OCT 2017

A Near-Global Atmospheric Distribution of N_2O Isotopologues

Peter F. Bernath^{1,2} , Mahdi Yousefi³, Eric Buzan¹ , and Chris D. Boone²
¹Department of Chemistry and Biochemistry, Old Dominion University, Norfolk, VA, USA, ²Department of Chemistry, University of Waterloo, Waterloo, Ontario, Canada, ³Department of Physics, Old Dominion University, Norfolk, VA, USA

Abstract The distributions of the four most abundant isotopologues and isotopomers (N_2O , ^{15}NNO , N^{15}NO , and NN^{18}O) of nitrous oxide have been measured in the Earth's stratosphere by infrared remote sensing with the Atmospheric Chemistry Experiment (ACE) Fourier transform spectrometer. These satellite observations have provided a near-global picture of N_2O isotopic fractionation. The relative abundances of the heavier species increase with altitude and with latitude in the stratosphere as the air becomes older. The heavy isotopologues are enriched by 20–30% in the upper stratosphere and even more over the poles. These observations are in general agreement with model predictions made with the Whole Atmosphere Community Climate Model (WACCM). A detailed 3-D chemical transport model is needed to account for the global isotopic distributions of N_2O and to infer sources and sinks.

1. Introduction

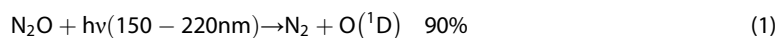
Nitrous oxide (N_2O) is an important greenhouse gas that contributes to climate change. Of the well-mixed greenhouse gases, N_2O is third in terms of radiative forcing after CO_2 and CH_4 (Intergovernmental Panel on Climate Change (IPCC), 2013). N_2O is essentially inert in the troposphere and has an atmospheric lifetime of about 120 years (Brown et al., 2013; Prather et al., 2015). In the stratosphere N_2O oxidation leads to the formation of NO_x (NO and NO_2), where it contributes to ozone destruction. The Montreal Protocol limits the use of ozone-depleting substances such as chlorofluorocarbons but does not address the increasing amounts ($\sim 0.25\%$ per year) of N_2O (Ravishankara et al., 2009). N_2O has a wide variety of surface sources but is primarily produced as a by-product of microbial nitrification and denitrification processes in soils and oceans. The 20% increase in the tropospheric volume mixing ratio (VMR) from the preindustrial value of 270 ppb to the 2011 value of 324 ppb is attributed mainly to modern agricultural practices through the application of nitrogen-containing fertilizers to crops (IPCC, 2013). The current 2017 VMR value is 330 ppb measured at Mauna Loa, Hawaii, by the NOAA/ESRL halocarbons in situ program.

Recent observations from the Atmospheric Chemistry Experiment (ACE) satellite (Semeniuk et al., 2008; Sheese et al., 2016) have led to the discovery of upper atmospheric N_2O sources from chemical reactions initiated by energetic particle bombardment. These particles form N atoms and excited metastable N_2^* , which lead to the formation of N_2O via the $\text{N} + \text{NO}_2$ and $\text{N}_2^* + \text{O}_2$ reactions. Descent of the N_2O product to the stratosphere leads to ozone depletion, particularly over the winter pole.

Isotopically substituted molecules (isotopologues) provide additional information on the chemistry and dynamics of atmospheric N_2O ; isotopologue abundances also constrain N_2O sources (Snider et al., 2015; Stein & Yung, 2003; Toyoda et al., 2013). The three most abundant stable minor isotopologues and isotopomers are ^{15}NNO , N^{15}NO , and NN^{18}O with natural abundances of about 0.36%, 0.36%, and 0.20%, respectively, with a parent $^{14}\text{N}^{14}\text{N}^{16}\text{O}$ abundance of 99%. Note that ^{15}NNO and N^{15}NO technically are the same isotopologue (singly substituted by ^{15}N) but are distinct isotopomers because they differ in the location of the isotopic substitution. Isotopologue and isotopomer abundances can be measured by isotope mass spectrometry (Kaiser, Röckmann, & Brenninkmeijer, 2003) and infrared absorption spectroscopy (Griffith et al., 2009, 2000). In general, the relative tropospheric abundances of the heavier isotopes have decreased with time as agricultural practices favor the production of the lighter parent molecule (Bernard et al., 2006; Ishijima et al., 2007).

In situ flask sampling from balloons and aircraft (e.g., Kaiser et al., 2006) with subsequent mass spectrometric analysis on the ground and high-resolution infrared solar absorption spectroscopy from balloon platforms (Griffith et al., 2000) find that the heavier isotopes are enriched at high altitudes as the N_2O concentration

decreases. This isotopic fractionation is caused by each isotopologue having a slightly different rate constant for the N_2O destruction reactions (McLinden et al., 2003; Yung & Miller, 1997):



in which the accepted relative contributions to removal are indicated as percentages (Burkholder et al., 2015; Minschwaner et al., 1993). The main source of $\text{O}(^1\text{D})$ in the upper atmosphere is the photolysis of ozone, and reaction (3) is responsible for NO_x production and ozone destruction in the stratosphere via the catalytic NO_x cycle (Finlayson-Pitts & Pitts, 2000). It has been suggested that reaction (1) is primarily responsible for the observed isotopic fractionation (Yung & Miller, 1997) and modern ab initio calculations of this fractionation (Schmidt et al., 2011) generally agree with laboratory and atmospheric observations.

The existing atmospheric observations of N_2O isotopologues are sparse, and global VMR distributions as a function of latitude and altitude are poorly known. Satellite measurements can provide near-global coverage not possible from in situ, balloon, and aircraft platforms. We report on infrared observations of the parent N_2O molecule and the first global observation of the three main minor isotopologues by the Atmospheric Chemistry Experiment (ACE) Fourier transform spectrometer (FTS) in low Earth orbit.

2. ACE Satellite Data

The ACE satellite (also known as SCISAT) is a Canadian mission for remote sensing of the Earth's atmosphere (Bernath, 2017; Bernath et al., 2005). It was launched by NASA into a near-circular orbit (altitude 650 km, inclination 74° to the equator) in August 2003 and is still active. The primary ACE instrument is a high spectral resolution (0.02 cm^{-1}) FTS operating from 750 to $4,400 \text{ cm}^{-1}$ (2.2 to $13.3 \mu\text{m}$). A sequence of atmospheric transmission spectra in the limb geometry is recorded using the Sun as an infrared source during sunrise and sunset (solar occultation technique). The satellite data are converted into altitude profiles of the volume mixing ratios (VMRs) of more than 35 trace gases and 20 isotopologues (as well as temperature and pressure) in version 3.5 of the processing (Boone et al., 2005, 2013). The N_2O line parameters from HITRAN 2012 were used (Rothman et al., 2012). The vertical resolution is about 3 km starting at 5 km altitude (or the cloud tops) and extending up to 95 km for N_2O and about 45 km for the ^{15}NNO , N^{15}NO , and NN^{18}O isotopologues. A maximum of 30 occultations are recorded per day with a "butterfly" sampling pattern (85°S – 85°N) as shown in Figure 6 of Bernath (2017), with near-global coverage about every 2 months. More details on ACE retrievals are provided in Text S1 in the supporting information.

3. Results

More than 30,000 occultations are available for the 2004–2013 period in version 3.5, and they were divided into four seasons (Figure 1). The satellite orbit leads to a concentration of measurements at high latitudes near about 60°N and 60°S .

The ACE N_2O isotopic data set contains a large amount of unphysical data when compared to other molecules. Several steps were taken to remove this bad data and improve the final results. First, data flagged as outliers by analysis from Sheese et al. (2015) are removed (data flagged as 1 and 2 were kept; for flags 4–7, the entire profile was removed). This reduced the number of occultations from 32,024 to 28,689. Next, profiles containing a negative VMR value are removed. While negative concentrations are allowed in ACE retrievals, they are not valid when calculating delta values. This further reduced the number of occultations used to 17,183. Finally, filtering using the median absolute deviation (MAD) was performed on the data points. MAD is defined as

$$\text{MAD} = \text{median}_i(|x_i - \text{median}_j(x_j)|) \quad (x)$$

and is less sensitive than the standard deviation to extreme outliers. The data set was binned by season, 10° latitude, and each altitude level and a MAD was calculated for each bin. Values with an

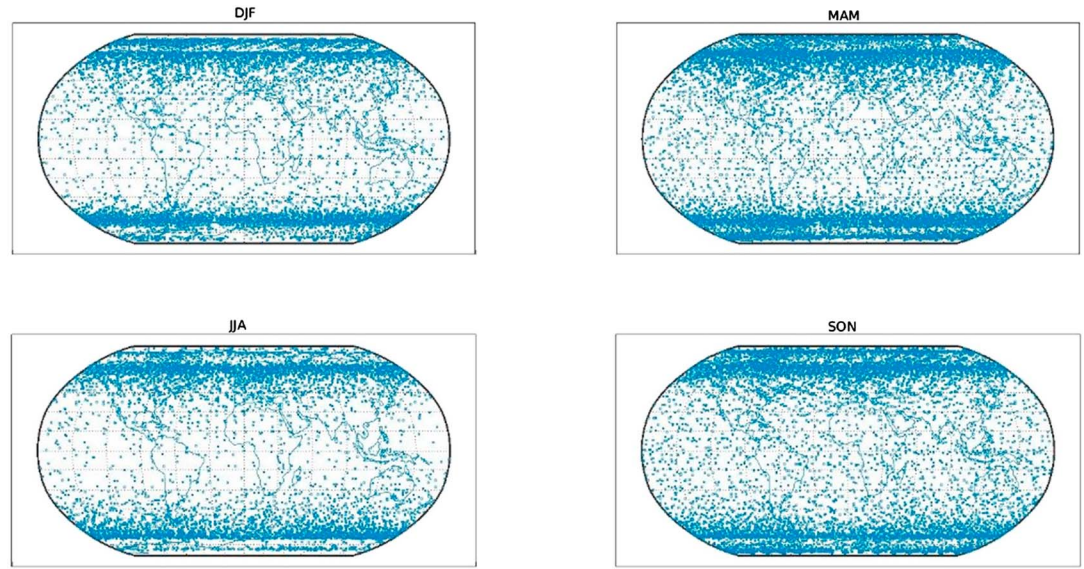


Figure 1. Distribution of ACE measurements by season (winter: DJF, December–February; spring: MAM, March–May; summer: JJA, June–August; and fall: SON, September–November).

absolute deviation higher than the MAD multiplied by 5 were discarded. This did not remove any full profiles.

After filtering nonphysical data, the δ values are calculated for each isotopologue as

$$\delta^{15}\text{N}^i = \left(\frac{{}^{15}R_{\text{sample}}^i}{{}^{15}R_{\text{ref}}^i} - 1 \right) \times 1,000\text{‰} \quad (i = 1, 2) \quad (4)$$

$$\delta^{18}\text{O} = \left(\frac{{}^{18}R_{\text{sample}}}{{}^{18}R_{\text{ref}}} - 1 \right) \times 1,000\text{‰} \quad (5)$$

$${}^{15}R^1 = \frac{[{}^{15}\text{N}^{14}\text{N}^{16}\text{O}]}{[{}^{14}\text{N}^{14}\text{N}^{16}\text{O}]}, \quad (6)$$

$${}^{15}R^2 = \frac{[{}^{14}\text{N}^{15}\text{N}^{16}\text{O}]}{[{}^{14}\text{N}^{14}\text{N}^{16}\text{O}]}, \quad (7)$$

$${}^{18}R = \frac{[{}^{14}\text{N}^{14}\text{N}^{18}\text{O}]}{[{}^{14}\text{N}^{14}\text{N}^{16}\text{O}]}, \quad (8)$$

in which ${}^{15}R_{\text{ref}} = 0.00367666$ and ${}^{18}R_{\text{ref}} = 0.002005$ are, respectively, the reference isotope ratio of air N_2 for nitrogen and Vienna standard mean ocean water for oxygen isotope measurements; ${}^{15}\text{N}^1$ refers to ${}^{15}\text{NNO}$, ${}^{15}\text{N}^2$ refers to N^{15}NO , and ${}^{18}\text{O}$ refers to NN^{18}O .

The ACE δ values in the troposphere were compared to in situ values measured on the ground, and small calibration factor of 0.9995 was applied to the isotopologue R values, based on in situ tropospheric values (see below). The ACE observations (Figure 1) were averaged in 10° latitude bins on a 1 km altitude grid for each

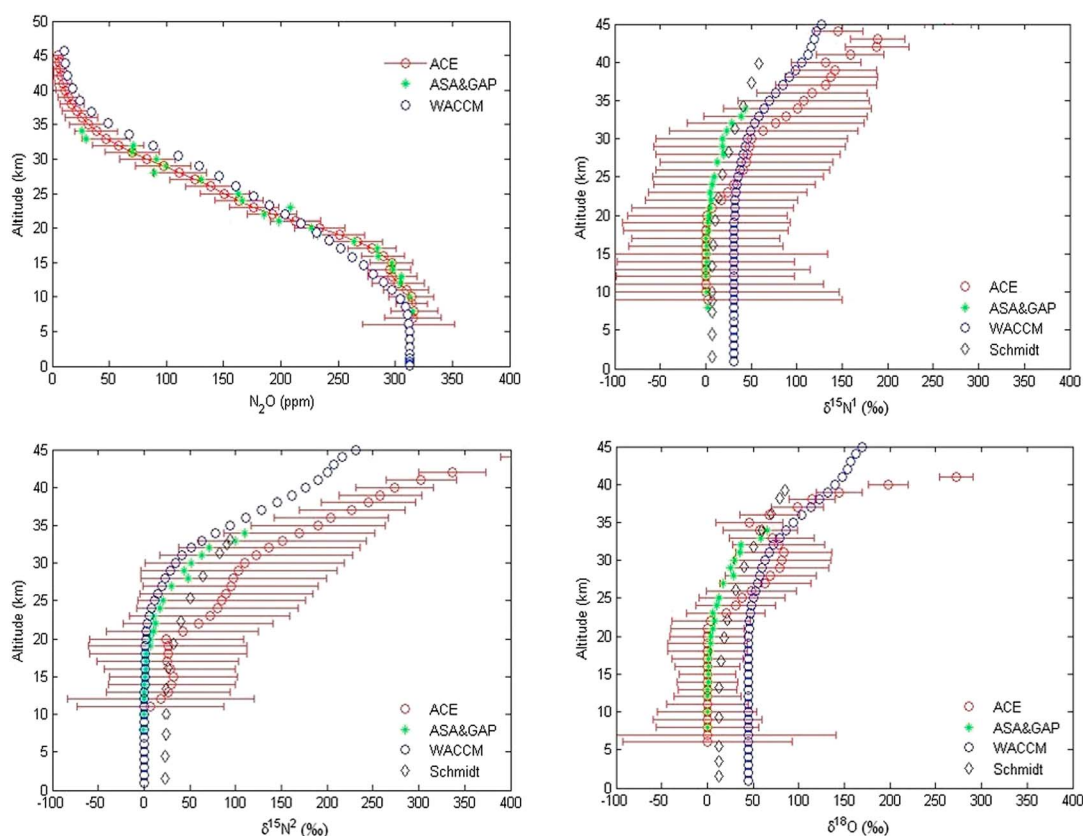


Figure 2. In the top left, the mission average ACE VMR profile for N_2O in the 40° – 50° latitude band, colocated predictions of WACCM and the average values measured over France with four high-altitude balloon flights (Kaiser et al., 2006). The other three panels show the corresponding δ values with one standard deviation error bars, as well as the midlatitude model values of Schmidt and Johnson (2015).

season and for the entire mission. As validation, the ACE δ values from the corresponding latitude bin were compared with in situ measurements (Kaiser et al., 2006) from high-altitude balloons (e.g., Figure 2). Figure 2 also displays the parent N_2O VMR profile. The expected relative increase in the heavier isotopologues with altitude as N_2O is photolyzed is observed, and good agreement is found between ACE and in situ balloon data.

The global distribution of δN values from ACE for the seasons is displayed in Figure 3 for $\delta^{15}\text{N}^2$, $\delta^{15}\text{N}^1$, and $\delta^{18}\text{O}$. The general pattern is the same for all three isotopologues: the heavier molecules are enriched in the stratosphere over the poles. The Brewer-Dobson circulation transfers older air with heavier isotopologues from the tropics to the poles. Moreover, Figure 3 shows the seasonal variation for the $^{15}\text{N}^1$, $^{15}\text{N}^2$, and ^{18}O isotopologues; in December–February and also March–May there is more sunlight over the South Pole that leads to enrichment of the heavier isotopologues (Figure 3). Similarly, over the North Pole the heavier isotopologues are enriched during June–August and September–November (Figure 3). It appears that the $^{15}\text{N}^2$ is slightly more enriched at lower altitudes than $^{15}\text{N}^1$; this can be explained by the ^{15}N site-dependent fractionation of the $^{15}\text{N}^1$ and $^{15}\text{N}^2$ isotopologues (Kaiser, Röckmann, Brenninkmeijer, & Crutzen, 2003).

4. Modeling

Model calculations were performed using version 4 of WACCM (Whole Atmosphere Community Climate Model), a component of the Community Earth System Model (Marsh et al., 2013). WACCM extends from the surface to 5×10^{-6} hPa (~ 140 km) and includes fully interactive chemistry and circulations patterns for the whole atmosphere. WACCM can be run as a stand-alone model or as the atmospheric component of CESM. This model was previously used for observing isotopologues of methane (Buzan et al., 2016) and CO (Beale et al., 2016), and a similar method is used here.

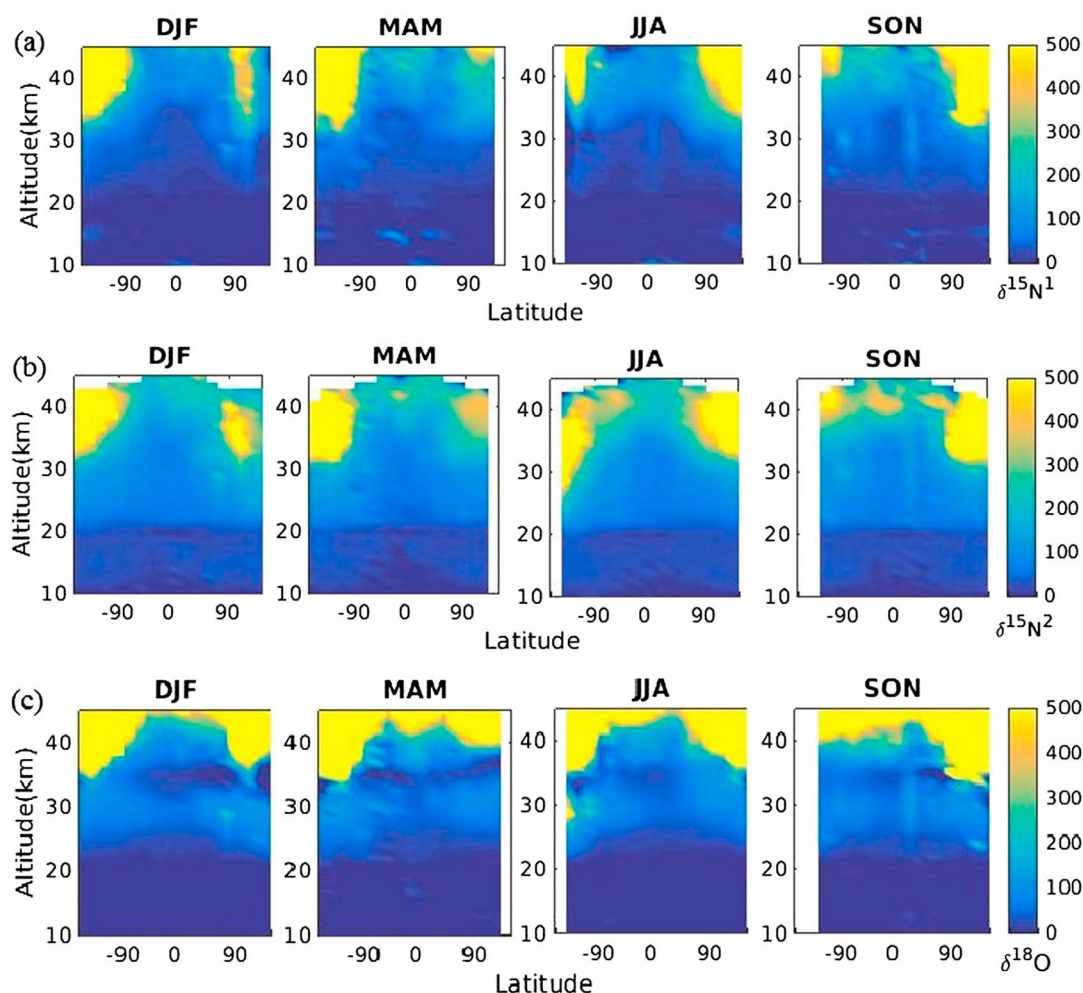


Figure 3. Observed ACE global distributions for (a) $\delta^{15}\text{N}^1$, (b) $\delta^{15}\text{N}^2$, and (c) $\delta^{18}\text{O}$.

Out of the box, WACCM does not support molecular isotopologues, but the isotopologues of N_2O can be inserted as separate species with a few modifications. First, the rate of the reaction of N_2O with $\text{O}(^1\text{D})$ is updated to the current Jet Propulsion Lab values (Burkholder et al., 2015) then adjusted by the kinetic isotope effects $\varepsilon = (k_{\text{Lighter}}/k_{\text{Heavier}} - 1) \times 1,000\text{‰}$, of each isotopologue (Kaiser, 2002). Next, new theoretical photolytic cross sections as a function of wavelength and temperature are added for each isotopologue (Schmidt et al., 2011). In this case the fractionation caused by different absorption cross sections (σ) is measured by $\varepsilon = (\sigma_{\text{Lighter}}/\sigma_{\text{Heavier}} - 1) \times 1,000\text{‰}$. Finally, tropospheric abundances of each isotopologue were inserted into the model by modifying WACCM's built-in surface boundary condition with δ values of tropospheric air measured by Röckmann and Levin (2005). Table 1 summarizes the above three values; here a single photolysis ε at 233 K and 200 nm is provided for comparison to the $\text{N}_2\text{O} + \text{O}(^1\text{D})$ reaction.

Table 1
Kinetic Isotope Effects for the Sinks of N_2O and Tropospheric Delta Values

Isotopologue	$\text{N}_2\text{O} + \text{O}(^1\text{D})$ $\varepsilon/\text{‰}$	Photolysis cross section ε (233 K, 200 nm)/ ‰	Tropospheric $\delta/\text{‰}$
$^{15}\text{N}^{14}\text{N}^{16}\text{O}$ (546)	+8.87	+30.63	+29.6
$^{14}\text{N}^{15}\text{N}^{16}\text{O}$ (456)	+2.22	+69.86	−16.2
$^{14}\text{N}^{14}\text{N}^{18}\text{O}$ (448)	+12.38	+40.97	+44.61

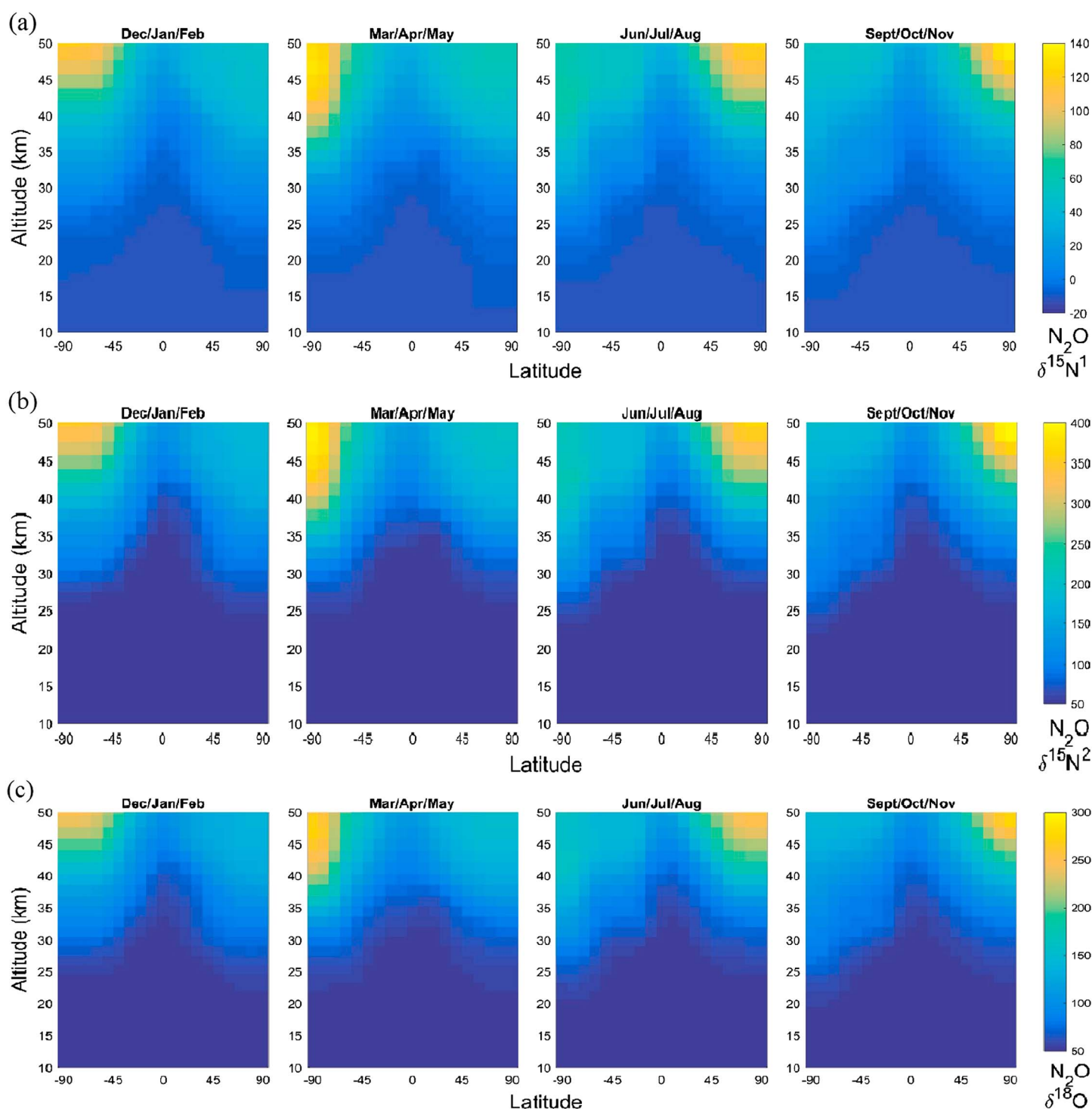


Figure 4. Seasonal WACCM data sampled at the ACE locations for (a) $\delta^{15}\text{N}^1$, (b) $\delta^{15}\text{N}^2$, and (c) $\delta^{18}\text{O}$.

WACCM was run as a stand-alone model with a resolution of $10 \times 15^\circ$ (latitude/longitude) and 66 vertical levels. The model was run as a perpetual year 2000 for a total of 120 years; the final 5 years were analyzed and compared to the ACE data set. The model data were corrected for the sampling bias from ACE by sampling WACCM's output as a series of "profiles" at the same location and time of year as the ACE profiles. The model data were separated by season and placed into 10° latitude bins to match that of ACE.

As shown in Figure 3, ACE and WACCM at midlatitudes (30–40°N) are in general agreement, although WACCM typically predicts less fractionation than observed by ACE. These disagreements are particularly noticeable near the top of the ACE retrieval range where the signal-to-noise ratio is low.

Figure 4 shows the model data for the δ values produced by WACCM for each of the three isotopologues. All three have similar features: increasing fractionation with altitude and toward the poles. The magnitude of fraction is highest for the $N^{15}NO$ isotopologue (Figure 1b), followed by $NN^{18}O$ (Figure 1c), and finally ^{15}NNO (Figure 1a). This trend matches the fractionation caused by photolysis, the primary sink of N_2O . Seasonal fluctuations are also present; enrichment of the heavy isotopologues is highest beginning in the summer and continuing over the fall (June–November in the Northern Hemisphere and December–May in the Southern Hemisphere). This is due to the increased sunlight, which drives photolysis. The seasonal variation is strong in the mesosphere and lower thermosphere and is only just visible at the top of the ACE data range.

However, this seasonal oscillation is less visible in the ACE data set. The sampled WACCM data set, shown in Figure 4, may explain why this occurs. The seasonal oscillation is diminished compared to the full WACCM data and only noticeable above 40 km. This is near 45 km, the altitude limit of the ACE data set where its measurements have the highest uncertainty.

In addition to the strong seasonal oscillation in the mesosphere, ACE is also not able to detect the isotopic signature due to N_2O production by the solar wind in the upper mesosphere and lower thermosphere. The chemistry associated with the solar wind was not included in WACCM but will create a unique isotopic signature.

The WACCM model predictions and ACE observations are in reasonable agreement with previous model results (Ishijima et al., 2015; McLinden et al., 2003; Yung & Miller, 1997), which also predict that the heavier isotopologues are enhanced in the stratosphere above the poles. As illustrated in Figure 6 of Ishijima et al. (2015), the sparse balloon data of Kaiser et al. (2006) also suggests a similar latitude and altitude dependence as observed by ACE. The altitude profile of N_2O over Hyderabad, India (18°N, 79°E), shows little fractionation, while those over Kiruna, Sweden (68°N, 26°E), and Showa, Antarctica (69°S, 40°E), show strong relative enrichment of the heavier isotopologues in the stratosphere. Recent in situ balloon observations by Toyoda et al. (2017) confirm that fractionation is relatively small in the tropics. This is expected given the more rapid decline with altitude of the N_2O VMR over the poles than in the tropics. The calculations of Schmidt and Johnson (2015) for midlatitudes (Figure 2) also show the expected moderate fractionation with altitude. This enrichment is a measure of the age of air: polar air in the stratosphere is older, N_2O is more photolyzed, and the heavier isotopologues are therefore relatively enriched. Indeed, ACE observations of N_2O isotopologues could be used as tracers to evaluate or perhaps infer the age of air (Waugh & Hall, 2002).

These global observations have implications for high precision isotopic N_2O analysis in the troposphere used to determine fluxes from various sources (e.g., Toyoda et al., 2013). Each source has a characteristic isotopic ratio and, for example, emissions from soils are depleted in ^{15}N (Toyoda et al., 2013). N_2O has such a long lifetime that the heavy isotopologue enhancement in the stratosphere affects the tropospheric δ value. The Brewer-Dobson circulation transports the fractionated gas poleward and downward with some heavily fractionated N_2O returning to the troposphere. The global ACE distributions of N_2O δ values highlight the importance of using a full 3-D chemical transport model to infer sources and sinks. In addition, the upper atmosphere source of N_2O could contribute to isotopic fractionation, especially in the winter as air from the upper atmosphere descends over the poles.

5. Conclusions

Spectroscopic observations from low Earth orbit with the ACE-FTS have given a global picture of the isotopic fractionation of nitrous oxide in the upper troposphere and stratosphere. The heavier isotopologues and isotopomers (^{15}NNO , $N^{15}NO$, and $NN^{18}O$) are enriched with increasing altitude and increasing latitude in the stratosphere. As confirmed by modeling with WACCM, the photolysis of N_2O in the near UV region is responsible for this pattern. As the air ages, there is a longer time for photolysis, a decrease in N_2O VMR and an increase in the relative abundance of the heavier N_2O isotopologues. The model predicts a strong seasonal variation over the poles in the mesosphere with the highest fractionation in sunlit summer pole and an amplitude that decreases with altitude.

Acknowledgments

The ACE mission is supported primarily by the Canadian Space Agency. We thank T. Röckmann for providing balloon profile measurements. Numerical values used to prepare Figures 3 and 4 are available as supporting information. The ACE-FTS Level 2 data used in this paper can be obtained through the ACE website (registration required), <http://www.ace.uwaterloo.ca>.

References

- Beale, C. A., Buzan, E. M., Boone, C. D., & Bernath, P. F. (2016). Near-global distribution of CO isotopic fractionation in the Earth's atmosphere. *Journal of Molecular Spectroscopy*, 323, 59–66. <https://doi.org/10.1016/j.jms.2015.12.005>
- Bernard, S., Röckmann, T., Kaiser, J., Barnola, J.-M., Fischer, H., Blunier, T., & Chappellaz, J. (2006). Constraints on N₂O budget changes since pre-industrial time from new firn air and ice core isotope measurements. *Atmospheric Chemistry and Physics*, 6(2), 493–503. <https://doi.org/10.5194/acp-6-493-2006>
- Bernath, P. F. (2017). The Atmospheric Chemistry Experiment (ACE). *Journal of Quantitative Spectroscopy and Radiation Transfer*, 186, 3–16. <https://doi.org/10.1016/j.jqsrt.2016.04.006>
- Bernath, P. F., McElroy, C. T., Abrams, M. C., Boone, C. D., Butler, M., Camy-Peyret, C., ... Zou, J. (2005). Atmospheric Chemistry Experiment (ACE): Mission overview. *Geophysical Research Letters*, 32, L15501. <https://doi.org/10.1029/2005GL022386>
- Boone, C. D., Nassar, R., Walker, K. A., Rochon, Y., McLeod, S. D., Rinsland, C. P., & Bernath, P. F. (2005). Retrievals for the atmospheric chemistry experiment Fourier-transform spectrometer. *Applied Optics*, 44(33), 7218–7231. <https://doi.org/10.1364/AO.44.007218>
- Boone, C. D., Walker, K. A., & Bernath, P. F. (2013). Version 3 retrievals for the Atmospheric Chemistry Experiment Fourier transform spectrometer (ACE-FTS). In *The Atmospheric Chemistry Experiment ACE at 10: A solar occultation anthology* (pp. 103–127). Hampton, VA: A. Deepak Publishing.
- Brown, A. T., Volk, C. M., Schoeberl, M. R., Boone, C. D., & Bernath, P. F. (2013). Stratospheric lifetimes of CFC-12, CCl₄, CH₄, CH₃Cl and N₂O from measurements made by the Atmospheric Chemistry Experiment-Fourier transform spectrometer (ACE-FTS). *Atmospheric Chemistry and Physics*, 13(14), 6921–6950. <https://doi.org/10.5194/acp-13-6921-2013>
- Burkholder, J. B., Sander, S. P., Abbatt, J., Barker, J. R., Huie, R. E., Kolb, C. E., ... Wine, P. H. (2015). *Chemical kinetics and photochemical data for use in atmospheric studies, evaluation no. 18*. Pasadena: JPL Publication 15–10, Jet Propulsion Laboratory. <http://jpldataeval.jpl.nasa.gov>
- Buzan, E. M., Beale, C. A., Boone, C. D., & Bernath, P. F. (2016). Global stratospheric measurements of the isotopologues of methane from the atmospheric chemistry experiment Fourier transform spectrometer. *Atmospheric Measurement Techniques*, 9(3), 1095–1111. <https://doi.org/10.5194/amt-9-1095-2016>
- Finlayson-Pitts, B. J., & Pitts, J. N. Jr. (2000). *Chemistry of the upper and lower atmosphere: Theory, experiments, and applications*. San Diego, CA: Academic Press.
- Griffith, D. W. T., Toon, G. C., Sen, B., Blavier, J.-F., & Toth, R. A. (2000). Vertical profiles of nitrous oxide isotopomer fractionation measured in the stratosphere. *Geophysical Research Letters*, 27(16), 2485–2488. <https://doi.org/10.1029/2000GL011797>
- Griffith, D. W. T., Parkes, S. D., Haverd, V., Paton-Walsh, C., & Wilson, S. R. (2009). Absolute calibration of the intramolecular site preference of ¹⁵N fractionation in tropospheric N₂O by FT-IR spectroscopy. *Analytical Chemistry*, 81(6), 2227–2234. <https://doi.org/10.1021/ac802371c>
- Intergovernmental Panel on Climate Change (IPCC) (2013). In T. F. Stocker et al. (Eds.), *Climate Change 2013: The Physical Science Basis. Contribution of Working Group I to the Fifth Assessment Report of the Intergovernmental Panel on Climate Change* (p. 1535). Cambridge, UK, and New York, NY: Cambridge University Press.
- Ishijima, K., Sugawara, S., Kawamura, K., Hashida, G., Morimoto, S., Murayama, S., ... Nakazawa, T. (2007). Temporal variations of the atmospheric nitrous oxide concentration and its ¹⁵N and ¹⁸O for the latter half of the 20th century reconstructed from firn air analyses. *Journal of Geophysical Research*, 112, D03305. <https://doi.org/10.1029/2006JD007208>
- Ishijima, K., Takigawa, M., Sudo, K., Toyoda, S., Yoshida, N., Röckmann, T., ... Nakazawa, T. (2015). *Atmospheric chemistry and physics discussions*, 15(14), 19,947–20,011. <https://doi.org/10.5194/acpd-15-19947-2015>
- Kaiser, J. (2002). Intramolecular ¹⁵N and ¹⁸O fractionation in the reaction of N₂O with O(¹D) and its implications for the stratospheric N₂O isotope signature. *Journal of Geophysical Research*, 107(D14), 4214. <https://doi.org/10.1029/2001JD001506>
- Kaiser, J., Röckmann, T., & Brenninkmeijer, C. A. M. (2003). Complete and accurate mass-spectrometric isotope analysis of tropospheric nitrous oxide. *Journal of Geophysical Research*, 108(D15), 4476. <https://doi.org/10.1029/2003JD003613>
- Kaiser, J., Röckmann, T., Brenninkmeijer, C. A. M., & Crutzen, P. J. (2003). Wavelength dependence of isotope fractionation in N₂O photolysis. *Atmospheric Chemistry and Physics*, 3(2), 303–313. <https://doi.org/10.5194/acp-3-303-2003>
- Kaiser, J., Engel, A., Borchers, R., & Röckmann, T. (2006). Probing stratospheric transport and chemistry with new balloon and aircraft observations of the meridional and vertical N₂O isotope distribution. *Atmospheric Chemistry and Physics*, 6(11), 3535–3556. <https://doi.org/10.5194/acp-6-3535-2006>
- Marsh, D. R., Mills, M. J., Kinnison, D. E., Lamarque, J.-F., Calvo, N., & Polvani, L. M. (2013). Climate change from 1850 to 2005 simulated in CESM1(WACCM). *Journal of Climate*, 26(19), 7372–7391. <https://doi.org/10.1175/JCLI-D-12-00558.1>
- McLinden, C. A., Prather, M. J., & Johnson, M. S. (2003). Global modeling of the isotopic analogues of N₂O: Stratospheric distributions, budgets, and the ¹⁷O–¹⁸O mass-independent anomaly. *Journal of Geophysical Research*, 108(D8), 4233. <https://doi.org/10.1029/2002JD002560>
- Minschwaner, K., Salawitch, R. J., & McElroy, M. B. (1993). Absorption of solar radiation by O₂: Implications for O₃ and lifetimes of N₂O, CFCl₃, and CF₂Cl₂. *Journal of Geophysical Research*, 98(D6), 10,543–10,561. <https://doi.org/10.1029/93JD00223>
- Prather, M. J., Hsu, J., DeLuca, N. M., Jackman, C. H., Oman, L. D., Douglass, A. R., ... Funke, B. (2015). Measuring and modeling the lifetime of nitrous oxide including its variability. *Journal of Geophysical Research: Atmospheres*, 120(11), 5693–5705. <https://doi.org/10.1002/2015JD023267>
- Ravishankara, A. R., Daniel, J. S., & Portmann, R. W. (2009). Nitrous oxide (N₂O): The dominant ozone-depleting substance emitted in the 21st century. *Science*, 326(5949), 123–125. <https://doi.org/10.1126/science.1176985>
- Röckmann, T., & Levin, I. (2005). High-precision determination of the changing isotopic composition of atmospheric N₂O from 1990 to 2002. *Journal of Geophysical Research*, 110, D21304. <https://doi.org/10.1029/2005JD006066>
- Rothman, L. S., Gordon, I. E., Babikov, Y., Barbe, A., Chris Benner, D., Bernath, P. F., ... Wagner, G. (2012). The HITRAN2012 molecular spectroscopic database. *Journal of Quantitative Spectroscopy and Radiation Transfer*, 130, 4–50.
- Schmidt, J. A., & Johnson, M. S. (2015). Clumped isotope perturbation in tropospheric nitrous oxide from stratospheric photolysis. *Geophysical Research Letters*, 42(9), 3546–3552. <https://doi.org/10.1002/2015GL063102>
- Schmidt, J. A., Johnson, M. S., & Schinke, R. (2011). Isotope effects in N₂O photolysis from first principles. *Atmospheric Chemistry and Physics*, 11(17), 8965–8975. <https://doi.org/10.5194/acp-11-8965-2011>
- Semeniuk, K., McConnell, J. C., Jin, J. J., Jarosz, J. R., Boone, C. D., & Bernath, P. F. (2008). N₂O production by high energy auroral electron precipitation. *Journal of Geophysical Research*, 113, D16302. <https://doi.org/10.1029/2007JD009690>
- Sheese, P. E., Walker, K. A., Boone, C. D., Bernath, P. F., & Funke, B. (2016). Nitrous oxide in the atmosphere: First measurements of a lower thermospheric source. *Geophysical Research Letters*, 43, 2866–2872. <https://doi.org/10.1002/2015GL067353>

- Snider, D. M., Venkiteswaran, J. J., Schiff, S. L., & Spoelstra, J. (2015). From the ground up: Global nitrous oxide sources are constrained by stable isotope values. *PLoS One*, *10*(3), e0118954. <https://doi.org/10.1371/journal.pone.0118954>
- Stein, L. Y., & Yung, Y. L. (2003). Production, isotopic composition, and atmospheric fate of biologically produced nitrous oxide. *Annual Review of Earth and Planetary Sciences*, *31*(1), 329–356. <https://doi.org/10.1146/annurev.earth.31.110502.080901>
- Toyoda, S., Kuroki, N., Yoshida, N., Ishijima, K., Tohjima, Y., & Machida, T. (2013). Decadal time series of tropospheric abundance of N₂O isotopomers and isotopologues in the Northern Hemisphere obtained by the long-term observation at Hateruma Island, Japan. *Journal of Geophysical Research: Atmospheres*, *118*(8), 3369–3381. <https://doi.org/10.1002/jgrd.50221>
- Toyoda, S., Yoshida, N., Morimoto, S., Aoki, S., Nakazawa, T., Sugawara, S., ... Ishijima, K. (2017). Vertical distributions of N₂O isotopocules in the equatorial stratosphere. *Atmospheric Chemistry and Physics Discussions*, 1–25. <https://doi.org/10.5194/acp-2017-272>
- Waugh, D. W., & Hall, T. M. (2002). Age of stratospheric air: Theory, observations, and models. *Reviews of Geophysics*, *40*(4), 1010. <https://doi.org/10.1029/2000RG000101>
- Yung, Y. L., & Miller, C. E. (1997). Isotopic fractionation of stratospheric nitrous oxide. *Science*, *278*(5344), 1778–1780. <https://doi.org/10.1126/science.278.5344.1778>